Correlations of heavy-flavour decay electrons with charged jets in pp collisions at $\sqrt{s} = 8$ TeV with ALICE

Diógenes Domenicis Gimenez for the ALICE Collaboration
University of São Paulo

Introduction

This analysis is based on a hadron-jet coincidence method [1], but a heavy-flavour observable is used instead of hadrons, since they are efficient probes to study the QGP (Quark-Gluon Plasma).

The heavy-flavour and jet observables are combined by selecting **heavy-flavour decay electron and charged-jet pairs** (HFe-Jet), creating a biased sample for studying their energy loss, exploiting the capabilities of ALICE (Fig.1) in electron identification. They can be also selected to be **back-to-back** (Fig. 2).

The data shown is from a Monte Carlo simulation of pp collisions at $\sqrt{s} = 8$ TeV. The selected events are triggered by the EMCal.

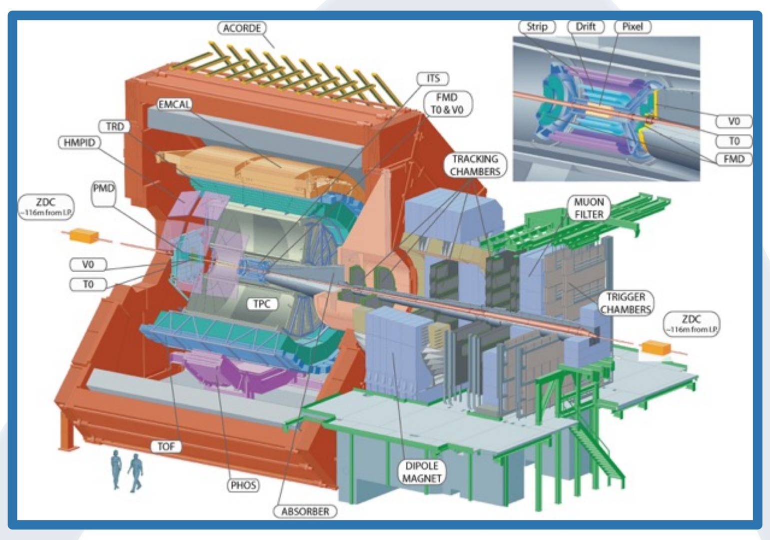

Fig.1 – ALICE detectors scheme. The ones used in this analysis are identified by their names: EMCal and TPC.

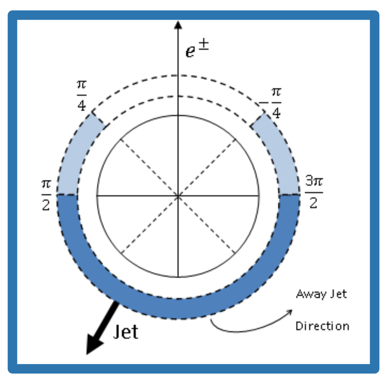

Fig.2 – Angles of jets, with respect to the electron, divided in ranges as used in this analysis.

Jet Reconstruction & Heavy-Flavour Decay Electron-Jet Correlation

The jet reconstruction uses:

- the **FastJet**[3] libraries;
- **anti-k_T** algorithm with $R = 0.4$.

The $N_{\rm jet}^{\rm HFe}$ properly **corrected** distribution is obtained following Eq.(3), taking into account also the efficiency of the selection $\epsilon_{\rm HFeID}$. The $N_{\rm jet}^{\rm HFe}$ can projected to $p_{\rm T,ch\,jet}$ for e-jet pair with $\Delta\varphi({\rm e,jet}) > \pi/2$ (away-side jets), or to $\boldsymbol{\Delta\varphi}(\mathbf{e,jet})$ integrating in $p_{\rm T,ch\,jet}$, as shown in Fig. 6. The used normalization is the number of identified electrons from heavy-flavour hadron decays.

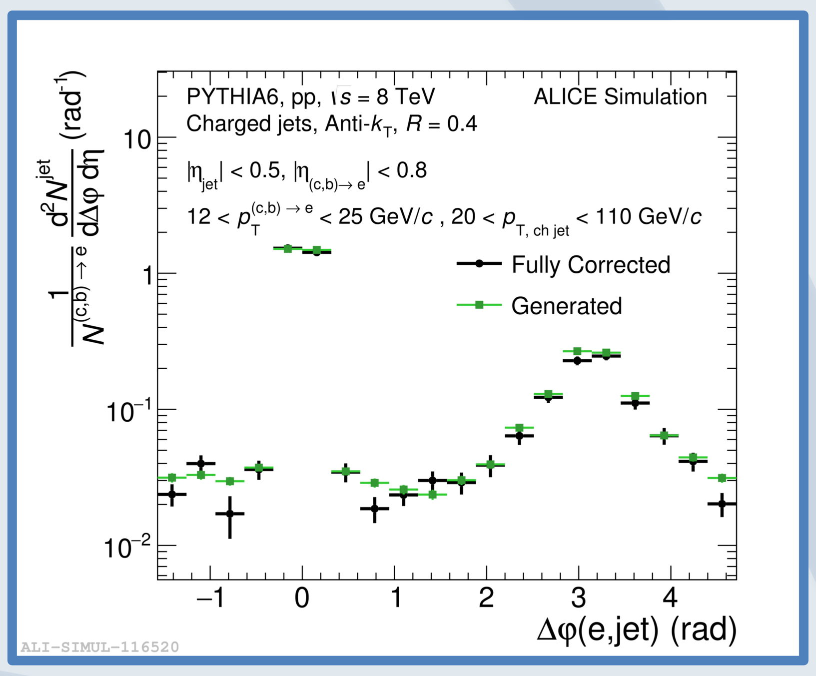

Fig.6 – HFe – Jet angular correlation. The corrected distribution (in black) is compared to the generated one (in green).

$$N_{\rm jet}^{\rm HFe} = \sum_{p_{\rm T}^{\rm e}} \frac{1}{\epsilon_{\rm HFeID}(p_{\rm T}^{\rm e})}\left\{N_{\rm e-jets}^{-1<N_{\sigma\,{\rm TPC}}^{\rm e}<3}(p_{\rm T}^{\rm e}) - f(p_{\rm T}^{\rm e})N_{\rm e-jets}^{-10<N_{\sigma\,{\rm TPC}}^{\rm e}<-3}(p_{\rm T}^{\rm e}) - \frac{(J_{\rm ULS}^{m<Cut} - J_{\rm LS}^{m<Cut})}{\epsilon_{m_{Inv}}(p_T^{\rm e})}\right\} \quad (3)$$

Unfolding

The jet $p_{\rm T}$ spectrum observable $N_{\rm jet}^{\rm HFe}$ must be unfolded in order to remove detector and algorithm effects, resulting in $\widetilde{N}_{\rm jet}^{\rm HFe}$. Iterative Bayesian RooUnfold [4] method is used.

In order to test the unfolding stability, the input $p_{\rm T}$ spectrum is **smeared** and **unfolded**.

- Smearing: Gaussian with $\sigma^{\rm Smear}$ as the input MC statistical uncertainty;
- Iterated 500 times;

A Gaussian is fit to the distribution (Fig. 7). The resulting $\sigma^{\rm fit}$ represents the stability of the method: variations within the input uncertainty result in unfolded spectra with uncertainties that are realistic with respect to the non-smeared unfolded spectrum.

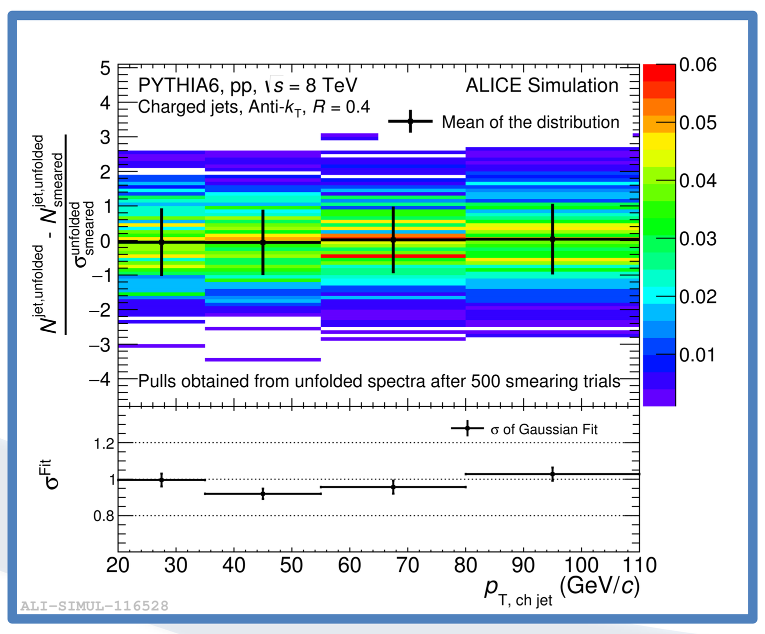

Fig.7 – [Upper panel] The pulls distribution for each $p_{\rm T,ch\,jet}$ bin is shown. The black points show the mean (and the RMS). [Lower panel] The Gaussian fit $\sigma^{\rm fit}$ is shown.

Outlook

The analysis chain is implemented and the next steps are:

- Analyse pp data at $\sqrt{s} = 8$ TeV;
- Analyse p-Pb data at $\sqrt{s_{\rm NN}} = 5.02$ TeV;
- Compare the results from the two systems, using as observable the nuclear modification factor $R_{\rm pPb}$;
- Analyse also Pb-Pb data at $\sqrt{s_{\rm NN}} = 5.02$ TeV (nuclear modification factor $R_{\rm AA}$).

Financial Support

FAPESP CNPq

Electron Identification

TPC specific energy loss, with respect to the expected for electrons (Eq. (1)), and **EMCal energy** information are used as follows:

- TPC cut is $N_{\sigma\,{\rm TPC}}^{\rm e} \in [-1,3]$;
- EMCal cut is $\frac{E}{p} \in [0.8,1.2]$;

Using both selections (Fig. 3), the purity of the selected particles is improved and also allows an estimate for the hadronic contamination (Fig. 4).

$$N_{\sigma\,{\rm TPC}}^{\rm e} = \frac{1}{\sigma_{\rm e}}\left[\frac{dE}{dx} - \left\langle\frac{dE}{dx}\right\rangle_{\rm e}\right] \quad (1)$$

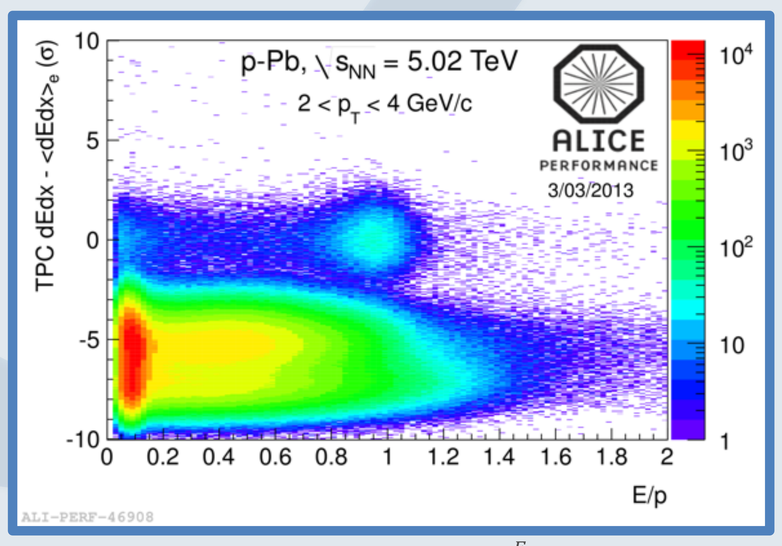

Fig.3 – Electron identification region in $\frac{E}{p} \times N_{\sigma\,{\rm TPC}}^{\rm e}$. This histogram data is from p-Pb collisions for tracks with $2 < p_{\rm T} < 4$ GeV/c

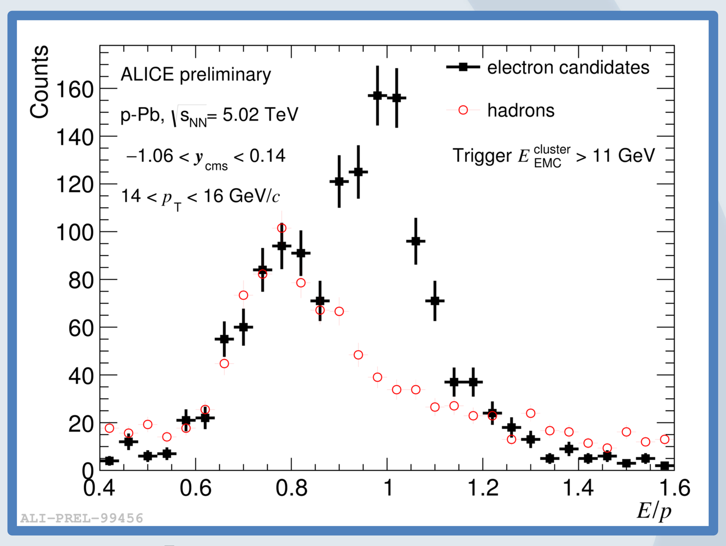

Fig.4 – $\frac{E}{p}$ distribution for electrons (in black, $-1 < N_{\sigma\,{\rm TPC}}^{\rm e} < 3$) and hadrons (in red, $-10 < N_{\sigma\,{\rm TPC}}^{\rm e} < -3$). The data shown are from p-Pb collisions for tracks with $14 < p_{\rm T} < 16$ GeV/c.

Hadronic Contamination

The E/p distribution is used to estimate the **hadronic contamination**. The distribution of jets correlated with the hadronic contamination $N_{\rm e-jets}^{-10<N_{\sigma\,{\rm TPC}}^{\rm e}<-3}$ is normalized, so the area in $0.6 < \frac{E}{p} < 0.8$ is the same as in the inclusive electrons one, $N_{\rm e-jets}^{-1<N_{\sigma\,{\rm TPC}}^{\rm e}<3}$, for each $p_{\rm T}^{\rm e} \times \Delta\varphi({\rm e,jet})$ bin. The contamination $f(p_{\rm T}^{\rm e})$ is the renormalized fraction in $0.8 < \frac{E}{p} < 1.2$.

Non-Heavy-Flavour Contamination

The electron selection includes also non-heavy-flavour decay electrons that must be subtracted:

- γ **conversions**;
- π^0 **Dalitz decay**.

In order to estimate it, the invariant mass (Fig. 5) is calculated for $\mathbf{e^\pm e^\mp}$ and $\mathbf{e^\pm e^\pm}$ pairs, with $m_{\rm Inv}^{\rm ee} < 0.135\,{\rm GeV}/c^2$. The contributions for $J_{\rm ULS}^{m<Cut}$ (Unlike-Sign pairs) and $J_{\rm LS}^{m<Cut}$ (Like-Sign pairs) are summarized in the Eq. (2), which shows that the **difference between them** results in the contamination. It is calculated for each $p_{\rm T}^{\rm e} \times \Delta\varphi({\rm e,jet})$ and summed, considering the efficiency $\epsilon_{m_{Inv}}$ of the method (Eq. (3)).

$$\begin{aligned} J_{\rm ULS}^{m<Cut} &= J_{\rm ULS,\,Non\,HFe}^{m<Cut,\rm Physical} + J_{\rm ULS,HFe-Comb}^{m<Cut} + J_{\rm ULS,Comb-Comb}^{m<Cut} \\ J_{\rm LS}^{m<Cut} &= J_{\rm LS,HFe-Comb}^{m<Cut} + J_{\rm LS,Comb-Comb}^{m<Cut} \end{aligned} \quad (2)$$

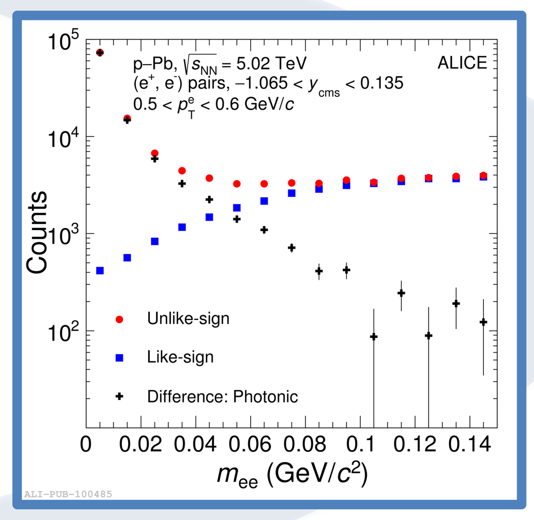

Fig.5 [2] – Invariant mass distribution for Like-Sign (LS) and Unlike-Sign (ULS) pairs. A peak in the ULS distribution, due to conversions, distribution is visible, under a certain threshold. The data used is from p-Pb collisions.

Jet Spectrum & Monte Carlo Information

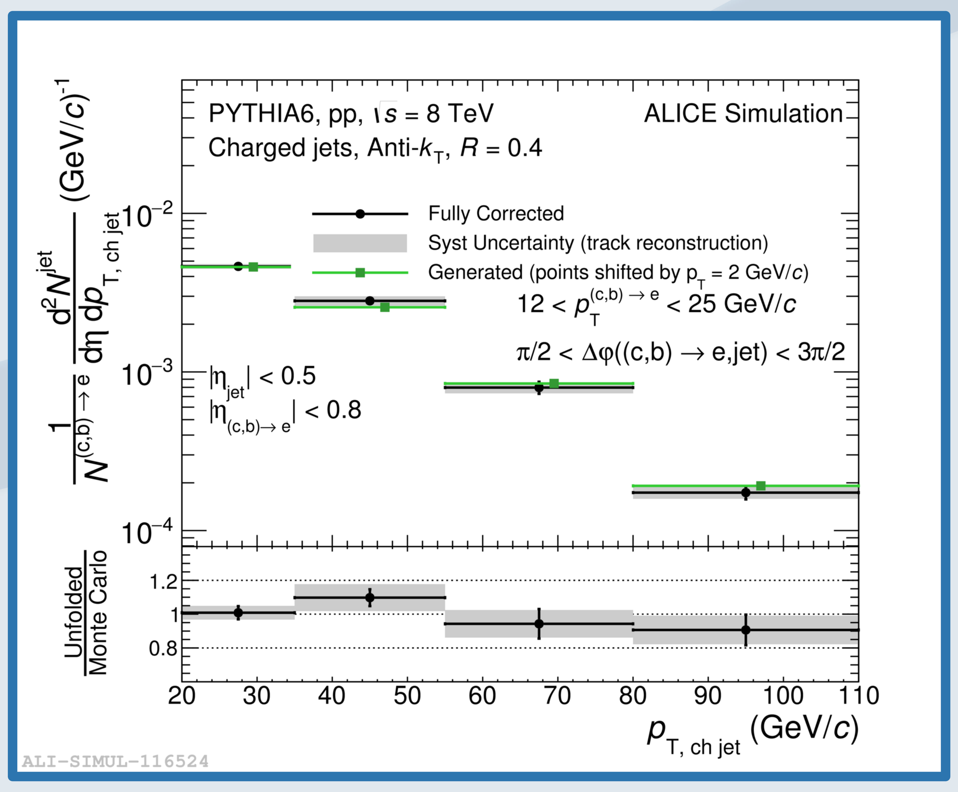

Fig.8 – Final HFe-Jet spectrum (in black) is compared to the normalized Monte Carlo truth one (in green). They are compatible within uncertainties.

The corrected, unfolded and normalized **away-side** charged jet spectrum is shown in Fig. 8, also comparing it to the Monte Carlo generated one.

The Monte Carlo information is the spectrum of jets reconstructed from generator-level particles correlated to true heavy-flavour decay electrons.

References

1. G. de Barros, B. Fenton-Olsen, P. Jacobs, and M. Ploskon, "Data-driven analysis methods for the measurement of reconstructed jets in heavy ion collisions at RHIC and LHC," Nucl. Phys. A910-911 (2013) 314–318, arXiv:1208.1518 [hep-ex]
2. ALICE Collaboration, "Measurement of electrons from heavy-flavour hadron decays in p-Pb collisions at $\sqrt{s}$=5.02 TeV", Phys. Lett. B 754 (2016) 81-93
3. M.Cacciari,G.P.Salam,G.Soyez,FastJet2.4.4 user manual (2010). URL http://fastjet.fr/
4. T. Adye "Unfolding algorithms and tests using RooUnfold" arXiv 1105.1160